

# Development of a wireless transmitter for in-core monitoring of reactor irradiation experiments

A.V. Fedorov\*, T.J. Schröder, A.S. Booij, D.N. Verbruggen, P.R. Hania, E. de Visser – Týnová  
NRG PALLAS, The Netherlands  
(\* ) fedorov@nrg.eu

**Abstract—** A wireless in-core radio transmitter which is currently under development at NRG-PALLAS will be able to amplify a signal measured inside a reactor core and transmit the signal to a receiver located outside the core without using instrumentation cables. The transmitter uses vacuum tubes as active components as these are judged – unlike transistors based on semi-conductors – to be able to withstand in-core radiation field. The transmitter is self- powered by means of a thermo-electric generator (TEG) utilizing nuclear heating present in the core.

A selection of electronic components envisaged to be used in the transmitter was irradiated in steps in a gamma field of 20 kGy/h reaching an accumulated irradiation dose of 720 kGy. The irradiation took place in the spent fuel pool of the High Flux Reactor (HFR). Relevant electronic properties of the components were measured before and after every irradiation step. The tested components included three types of miniature low anode voltage vacuum tubes, a variety of capacitors and resistors of different nominals, structures and compositions, and a bismuth telluride TEG unit.

In a next step electronic characteristics of vacuum tubes and capacitors were measured on-line during irradiation. These type of experiments were focused on the performance characteristics of the components in strong gamma field.

In all irradiation experiments the pre-selected electronic components behaved reasonably well and did not show any significant degradation of properties.

Details on the irradiation conditions and results of the measurements are presented.

**Keywords** — wireless in-core radio transmitter, self- powered, radiation resistant, vacuum tubes

## I. INTRODUCTION

CONTINUED development of new experimental methods and measuring techniques is crucial for successful conduction of irradiations performed at the High Flux Reactor (HFR) and in perspective in the future Pallas reactor which is currently under construction. In this respect self-powered wireless sensors that can precisely monitor process variables inside an operating nuclear reactor core, while withstanding its harsh radiation environment, are of great potential benefit. This technology has the potential to significantly reduce amount of

cables and number of penetrations in the reactor vessel, provide increased flexibility for installing various sensors, in particular in locations which are difficult to access through conventional methods. Wireless sensors are applicable for Material Research Reactors, Nuclear Power Plants and other nuclear facilities including fuel fabrication facilities and spent fuel storage installations [1][2][3][4].

In support of future irradiation experiments, NRG-PALLAS has started the RADIO (iRrADIAtIon technOlogy) project aiming to evaluate technical options of wireless transmission out of the core of a nuclear reactor during operation. The transmitter will be able to amplify a signal measured inside a reactor core and transmit the signal to a receiver located outside the core without using instrumentation cables. The transmitter uses vacuum tubes as active components as these are judged to be better suited to withstand in-core radiation field than transistors based on semi-conductors. The transmitter is self- powered by means of a thermo-electric generator (TEG) utilizing nuclear heating present in the core.

A similar approach was employed in the joint effort of Westinghouse and the Penn State University aiming to develop a self-powered wireless real-time reactor power sensor to measure core power peaking factor. The sensor uses a vacuum micro-electronic transmitter as active component which is powered by rhodium self-powered neutron sensor. The transmitter was tested in the Penn State TRIGA reactor reaching the neutron dose  $8.97 \times 10^{17}$  n/cm<sup>2</sup> and gamma dose 725 MRad (7.25MGy) [6][7].

The development of the self-powered wireless transmitter at NRG-PALLAS faced a number of challenges from which the main are related to the following aspects:

- **Radiation resistance of the electronic components:** wireless transmitter operated in radiation fields have to fulfil requirements on radiation resistance. In many cases, the requirements on radiation resistance of the used components raises the need to develop customized solutions. The results of the radiation tests performed within the project are presented in Section III.

- **Low frequency data transmission:** It was realized that to bridge the reactor vessel containment, application of very low frequencies (VLF; <30 kHz) will be required. The VLF range is technical challenging for several reasons, including low antenna sensitivity, large interferences in industrial

environments, and spatial limitations that hampers the implementation of efficient antennas [14]. Because the VLF range is usually avoided for communication purposes and only very few commercial solutions are available, often using large amounts of energy, the deployment of VLF technology in a reactor environment requires customized technical solutions for the electronic hardware, and careful evaluation and testing of feasible transmission frequencies. Application of low frequencies solutions through solid, electrically highly conductive media necessitates the use of magnetic fields which have a complex propagation behavior under near field and extended near field conditions. For the successful implementation of a low frequency transmitter located behind a significantly shielding barrier, and with a constrained supply of power, a good quantitative understanding of field generation and propagation through electrically conductive media is important. Results of the studies performed on magnetic field propagation in water and metals are presented in Section IV.

• **Technology development and integration:** an important aspect and key driver for the approach followed in this project is that none of the necessary components of the transmission chain is covered by the technological mainstream and the vast variety of technical solutions offered on the market. The development of an autonomous operating wireless sensor unit for the intended application is a complex and unique task, requiring multidisciplinary knowledge and experience in working fields that goes beyond material science and irradiation experiments: besides a good understanding of analog technology and application electronics in general, knowledge on communication technology and signal processing, and the physics of magnetic field propagation is necessary. Section V is focused on understanding the requirements of wireless in-core monitoring devices and translate this into creative and innovative solutions that allow to monitor under extreme harsh environmental conditions.

## II. EXPERIMENTAL

### A. Gamma Irradiation Facility

Radiation resistance of the electronic components were tested in the gamma field in the HFR spent fuel pool. A dedicated Gamma Irradiation Facility (GIF), shown in Fig. 1 and Fig. 2, was developed that allows to perform in-situ measurements of electronic components during the irradiations.

The irradiation experiments in the GIF facility were performed in two steps: first an initial screening of the radiation resistance of selected components was performed. For the components that passed, in a second step the behaviour under irradiation was studied in more detail. Together with these tests, a workflow and the necessary tooling was implemented and built, allowing to irradiate and test components efficiently under well-defined conditions.

Three irradiations were carried out. The irradiation parameters are shown in Table I. Irradiation A was performed in multiple steps (A1, A2 and A3). The irradiation B was performed in one step. For both irradiations the electronic characteristics of the irradiated components were measured before and after each irradiation step. These irradiations were focused on permanent

irradiation damage which increases with the dose and on its effect on electronic characteristics of the components under study. The maximum irradiation gamma dose achieved in these tests was 725 kGy.

Differently, irradiation test C was focused on measurements of characteristics of the electronic components during irradiation. The gamma dose rate in the irradiation C was 17.3 kGy/h, which corresponds to  $4.8 \times 10^{-3}$  W/g. A typical gamma heating in HFR is about 5 W/g, thus irradiations in the GIF facility can only discard electronic components with poor performance under irradiation conditions, but will not guarantee their operation in an in-core position.

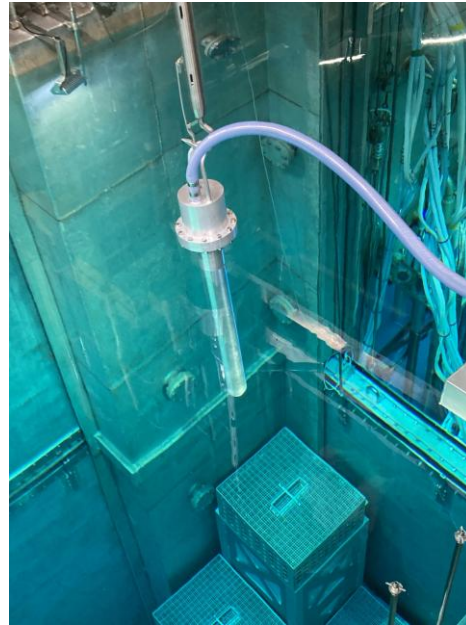


Fig. 1 Gamma irradiation facility with instrumentation cable in the HFR spent fuel pool.

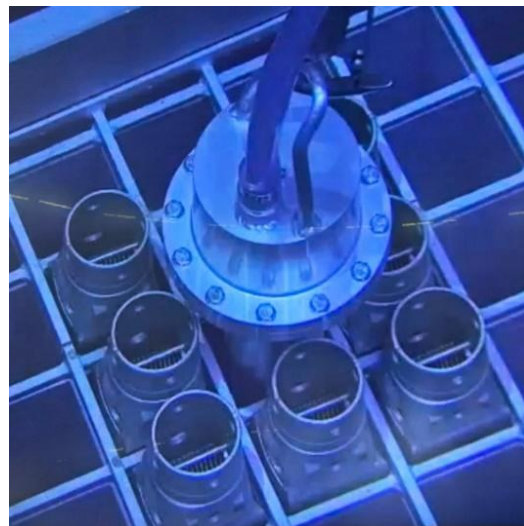


Fig. 2 Gamma irradiation facility in the irradiation position surrounded by spent fuel elements.

TABLE I  
PARAMETERS OF THE IRRADIATION EXPERIMENTS

No	Instrumented	Dose rate [kGy/h]	Accumulated dose [kGy]
A1	No	15.9	30
A2	No	15.9	90
A3	No	15.9	690
B	No	21.0	725
C	Yes	17.3	26

The electronic components under study included vacuum tubes, capacitors and resistors of different nominal values and different material composition and build, antenna wire with enamel insulation and a commercial thermo-electric generator. Electronic components are usually classified as passive or active components. Active components in this project are the vacuum tubes, while passive components include capacitors and resistors. The vacuum tubes chosen for the program were the miniature pentode tubes 1Zh37B and 1P24B (in two different making), with rod structure [8]. The rod structure of these tubes in contrast to commonly used grids offers extra robustness against vibrations. Both tubes run at low anode voltage,  $\sim 10$  V, which is a key feature enabling to power the transmitter with a low voltage TEG.

In the pre-selection of passive components most attention was focused on the materials in use and their radiation resistance. Materials as polymer film, paper and liquid electrolytes were directly excluded. Capacitors pre-selected for the irradiation tests contained dielectric materials such as glass, ceramic, mica, and oxide layers (As exception, one capacitor with polystyrene film as dielectric layer was present in the program). The main characteristics measured in the tests are the capacitance and leakage current. The nominal capacitance varied from 10 nF to 10  $\mu$ F. The capacitance was determined over a larger bandwidth to avoid problems with interferences on the long signal wiring used.

A variety of resistors of different makings with resistance values between 47 Ohm and 10 MOhm was preselected for tests. Both 'traditional' thru-hole-types with leads on both ends, and smaller 'Surface Mounting Devices' (SMD) without leads were included. Variety of tested resistive element included carbon, metal film and wire.

All electronic components were soldered on a Printed Circuit Board (PCB) as shown in Fig. 5. For the measurements, both standard apparatus and in-house made dedicated electronics were used.

The irradiation tests have also included a commercial  $40 \times 40$  mm bismuth telluride thermo-electric generator (TEG). The measured thermo-electric properties included thermo-electric force and internal resistance.

### B. Measurements of electro-magnetic field attenuation

To characterize frequency- and distance-dependent attenuation of magnetic field in water, a large bandwidth transmitter operating between 200 Hz and 9 kHz was developed. The transmitter is powered by low-voltage batteries, and provides an output voltage  $> 4$ V to the low ohm, inductive load of the transmitter antenna. Because these tests do not involve radiation

conditions the test-transmitter uses conventional semiconductor based electronics. The test-transmitter uses a D-class amplifier and a 40 cm diameter magnetic loop antenna. The receiving antenna is a 2 meter diameter loop antenna with a pre-amplifier and a data logger.

The underwater test was carried out in a test basin at NRG-PALLAS. The basin is 6 x 6 m wide and has a water depth of 4 m. Fig. 3 gives an overview of the experimental set-up with the test transmitter located in the middle of the basin and the receiver antenna floating in a coaxial position on the water, and the receiver electronics located on a desk beside the basin. During the measurements, the test transmitter was lowered in intervals of 50 cm, from 50 cm below the water line down to 4 m on the basin's floor. At each depth, signals from the transmitter between 200 Hz and 9 kHz were recorded.



Fig. 3. General set-up for underwater testing. The transmitter antenna is located close to the basin floor, and the receiver antenna is floating on top.

To study magnetic field propagation through a highly conductive slab of aluminium with a relevant thickness a desktop experiment was performed (see Fig. 4). In this experiment, the frequency-dependent signal transmission between two coaxial coils of 40 mm diameter was measured, separated by an aluminium plate of  $200 \times 400 \times 4$  mm.



Fig. 4. Measurement of magnetic field attenuation through a 4 mm slab of aluminum.

Furthermore, in preparation of future transmitter experiments, vertical and radial magnetic background noise and interferences in the HFR has been measured and characterized on several locations foreseen for the receiving antenna.

### III. RESULTS OF IRRADIATION TESTS

Material qualification experiments presented in this Section are focused on selection of suitable active and passive electronic components, and determination of the radiation resistance and performance of these components in a strong gamma field.

#### A. Vacuum tubes

PCB adapters with electronic components under study before and after irradiation are shown in Fig. 5. The borosilicate glass of the vacuum tubes have shown a red-brownish coloring, already clearly visible after the first 30 kGy of irradiation. This effect of radiation on glass is known in literature (e.g. [9][10]), but no impairment of the glass bulb's function was found in the irradiations.

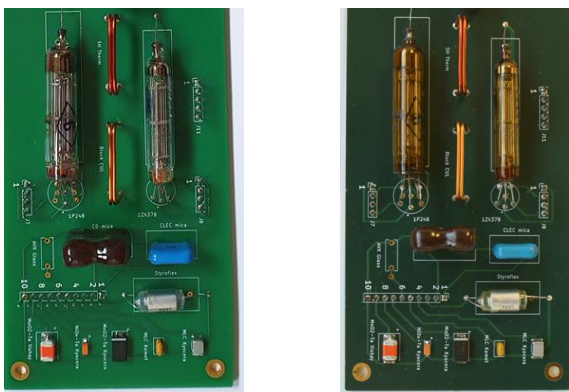


Fig. 5. PCB adapters with the vacuum tubes and capacitors under testing before irradiation (left) and after irradiation, 690 kGy (right).

The vacuum tubes were characterized by measuring the anode current as a function of grid voltage, at constant anode-cathode voltage (transfer function) [11][12]. Fig. 6 shows the transfer function measured for the vacuum tube 1P24B during and after irradiation with 17.3 kGy/h at 9 V anode voltage. The vacuum tubes showed only small deviations during and after irradiation, compared to production tolerances.

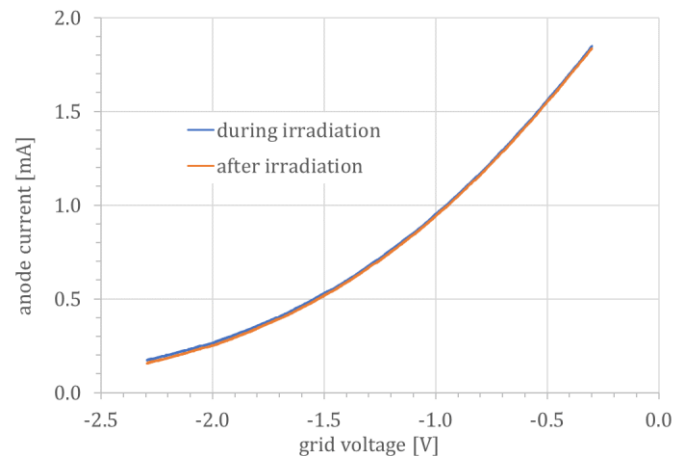


Fig. 6. The transfer function measured on the vacuum tube 1P24b during irradiation with a dose rate of 17.3 kGy/hr and after irradiation with about 26 kGy for an anode voltages of 9 V.

Two other important characteristics measured in the tests are filament current and saturated anodic current. No significant changes of the filament currents were found after irradiation at 725 kGy. The anodic current, however, was significantly decreased, by 21%, in one of the vacuum tubes (1P24B), pointing to chemical alterations of the filament's surfaces that decreases the electron emission efficiency. More detailed testing showed that this decrease is partially reversible by heating, raising the question if this decrease would also occur if the tube is operated during irradiation. The irradiation C with on-line measurements has strengthened this assumption: here, no decrease of the anodic current was found.

#### B. Capacitors

For a selected set of capacitors, the capacitance and leakage currents were measured. The capacitance was determined over a larger bandwidth.

Table II summarizes the measured capacity before and after 30, 90 and 690 kGy of irradiation. No significant change of the capacitance was found for two mica capacitors and one of the MLC (Multilayer Ceramic Capacitor) capacitor (MLC-1). The capacity of the polystyrene capacitor increased slightly (about 1%) after 690 kGy of irradiation. The MLC-2 showed a decrease of about 5% of its capacity. For the Ta-type capacitor a significant increase was found for all three tested versions already after 30 kGy. After 690 kGy, the MnO<sub>2</sub>-Ta-2 showed an increase of more than a factor of 5. The capacitance of the NbO-Ta capacitor increased by more than a factor of two. Despite the strong capacitance increase of some capacitor types, none of the capacitors showed a voltage breakthrough.

The objective of this irradiation tests was not to get understanding of the mechanisms responsible for degradation of the properties but rather to discard electronic components which behaved poorly in the tests from the further investigation.

TABLE II  
MEASURED CAPACITY BEFORE AND AFTER 30, 90 AND 690 kGy OF  
IRRADIATION

Type	Reference	30 kGy	90 kGy	690 kGy
Mica-1	9.89 nF	9.87 nF	9.89 nF	9.90 nF
Mica-2	9.95 nF	9.94 nF	9.96 nF	9.97 nF
Polystyrene	10.1 nF	10.1 nF	10.1 nF	10.2 nF
MLC-1	99.6 nF	99.6 nF	99.6 nF	99.6 nF
MLC-2	91.5 nF	88.6 nF	87.4 nF	86.6 nF
MnO <sub>2</sub> -Ta-1	10.7 μF	13.6 μF	23.1 μF	53.4 μF
MnO <sub>2</sub> -Ta-2	10.2 μF	10.9 μF	11.9 μF	16.2 μF
NbO-Ta	11.0 μF	12.2 μF	15.2 μF	24.4 μF

The capacitors which showed good performance in these irradiation tests, mica, polystyrene and MLC, were tested further in the irradiation C with on-line measurements. A capacitance measurement in broad frequency range performed on the MLC capacitor is shown in Fig. 7 and shows a good agreement between the measurement during irradiation and two reference measurements, before the irradiation and after. Similar results were obtained for mica and polystyrene.

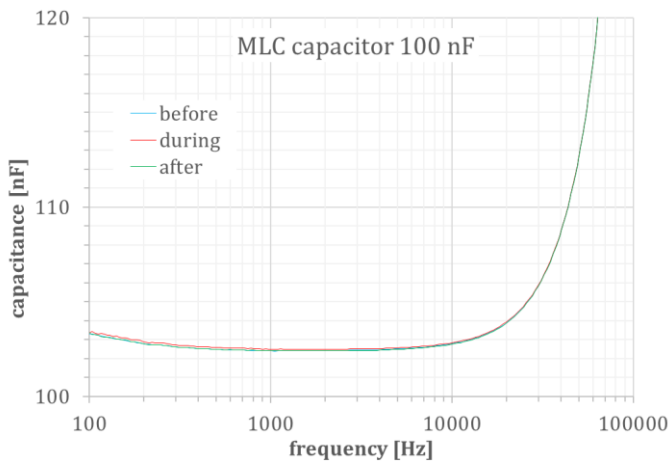


Fig. 7. Measured capacitance of the MLC capacitor measured before, during, and after irradiation.

The leakage currents measured on the tested capacitors during irradiation were  $\leq 4$  nA/V, which is sufficiently low for practical application, e.g. in an RCL-tank or as bias-blocking device. Unfortunately, but not unexpected, the larger capacitors with capacitances in the  $\mu$ F-range failed the irradiation tests and an alternative solution has to be found.

### C. Resistors

The selected resistor types showed no effects during the irradiation with 690 kGy in the GIF facility, allowing to select from a wide variety of resistor types and designs in the next steps. The results of the measurements are shown in Table III.

TABLE III  
MEASURED RESISTANCE BEFORE AND AFTER IRRADIATION

Type	Leads	Reference	690 kGy
Metal film-1	through hole	10 M $\Omega$	9.99 M $\Omega$
Metal film-2	through hole	47.2 $\Omega$	47.3 $\Omega$

Metal oxide	through hole	10.04 M $\Omega$	10.03 M $\Omega$
Thick film	SMD	10.03 M $\Omega$	10.03 M $\Omega$
Thin film	SMD	47.4 $\Omega$	47.4 $\Omega$
Carbon film	through hole	10.13 M $\Omega$	10.14 M $\Omega$
Thin film	SMD	10.01 M $\Omega$	10.01 M $\Omega$
Thick film	SMD	47.2 $\Omega$	47.3 $\Omega$
Thin film	SMD	47.4 $\Omega$	47.4 $\Omega$

### D. TEG

After the irradiation the ceramic surface of the TEG showed a slight yellowish-grey colouring. The measured thermoelectric force after irradiation was determined as 87.9 mV/ $^{\circ}$ C without load, this is within 4% of the value given in the datasheet (91.2 mV/ $^{\circ}$ C for a  $\Delta T$  of 170 $^{\circ}$ C). 53.4 mV/ $^{\circ}$ C was measured with a 10 Ohm load, resulting in an estimated internal resistance under load conditions of about 6.5 Ohm, which is lower than the 9.5 Ohm  $\pm 15\%$  given in the datasheet, but consistently within 4% of the thermal force given in the datasheet, considering the estimated internal resistance correct. Thus, it can be concluded that the TEG's thermal force after the irradiation is well within the value provided in the datasheet, considering that thermal coupling of the device can introduce experimental errors of 10%. Finally, the thermo-electric performance of the TEG was within specifications after irradiation, pointing to limited or no permanent damage.

The PCB showed no impairment of its basic function and is found to be suitable for the applied radiation conditions. The observed colouring of the solder mask does not impair the performance of the PCB. For future irradiation experiments with a much higher irradiation dose, however, it could be considered to manufacture a PCB without the solder mask.

## IV. PROPAGATION OF ELECTROMAGNETIC FIELD IN WATER AND METALS

Signal from an in-core radio transmitter has to propagate through the wall of the reactor core and several meters of water of the reactor pool. In case of HFR that would be 5 cm of aluminum (AA5451) and 8 meter of fresh water. Therefore, propagation of radio waves in low frequency range through relevant media (water, air, aluminum, Zircaloy, stainless steel) was essential part of the investigation.

Propagation of electro-magnetic field in water has been studied in the test basin at NRG-PALLAS site as described in Section II.B. Fig. 8 summarizes the outcome of the measurements as a function of the transmission distance. Within the investigated frequency range the observed attenuation of the signal strength is essentially due to the geometry factor, and no significant signal attenuation in ultrapure water of the basin was observed.

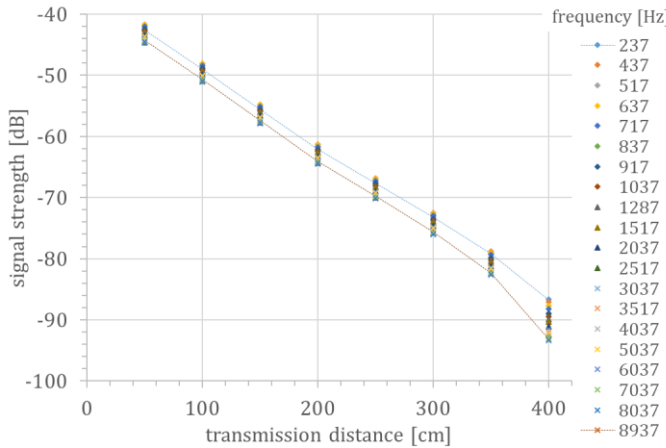


Fig. 8. Signal strength as a function of the transmission distance for frequencies between 200 Hz and 9 kHz

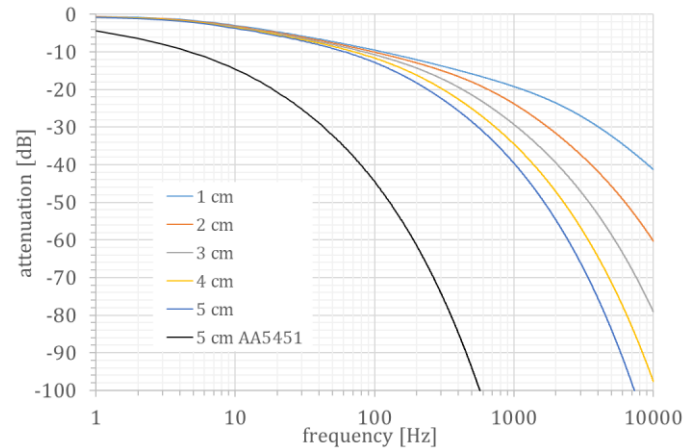


Fig. 10. Calculated signal strength for 1 to 5 cm of SS 301 or Zircaloy and 5 cm of AA5451 for the frequency range 1 Hz to 10 kHz.

Propagation of electro-magnetic field in aluminum has been studied using the setup described in Section II.B. Attenuation as a function of the frequency is shown in Fig. 9.

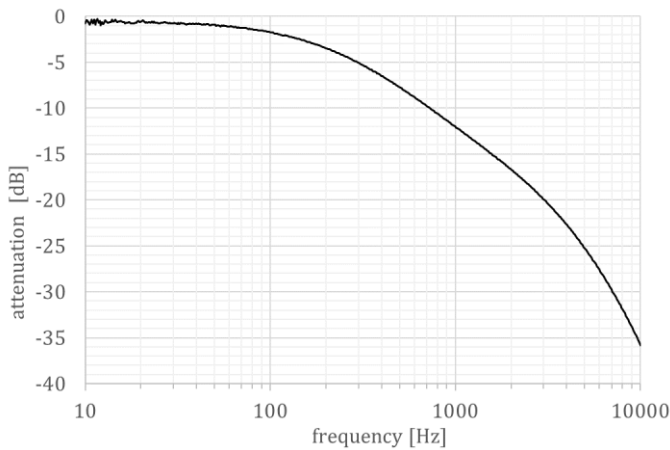


Fig. 9. Measured signal attenuation of magnetic fields by a 4 mm aluminum slab.

The propagation behaviour's dependency on the slab's thickness ( $t$ ) is roughly defined by the product of  $t \cdot \sqrt{\omega}$ , allowing to scale the thickness of the slab by invers scaling of the frequency ( $\omega$ ): upscaling of the above measurement by 12:1 would then represent a slab thickness comparable to the 5 cm of the HFR reactor wall [13][14].

This approach allows to make first principal analyses of the signal attenuation to be expected in the HFR, or other reactor designs as the future Pallas reactor. Fig. 10 shows the frequency-dependent attenuation of magnetic fields through 5 cm of aluminium as present in the HFR, and through 1 - 5 cm of SS 301 or Zircaloy-4. The results clearly show that reactor vessels made from less conductive metals than aluminium allow transmitting at technically more suitable frequencies, with less than 40 dB attenuation at 1 kHz.

## V. WIRELESS SENSOR UNIT

A wireless monitoring solution consists of several parts. In the first step of the transmission chain, data from a sensor is coded by modulating its information on a fixed carrier frequency. This signal is usually a voltage signal that needs to be amplified to provide sufficient current to the transmitting antenna. The amplified signal is then injected into the transmitter antenna, located at wall of the reactor vessel. The magnetic field build up by the transmitter antenna propagates through the reactor wall and induces a voltage in the receiver antenna. The voltage is then amplified and filtered, and the sensor data is extracted from the resulting signal thereafter.

The most critical element of the above set-up is the in-core transmitter, as the receiver is located outside the reactor basin and its technology can rely on a wide variety of available hardware and software solutions. The in-core transmitter can be envisioned as an autonomous operating Wireless Sensor Unit (WSU), with the core components depicted in Fig. 11.

The essential part of the wireless sensor unit is the oscillator providing the carrier frequency. In 2020 a proof-of-principle lab experiment was realised in which an oscillator built on a vacuum tube 1Zh37B was powered by a bismuth telluride commercial TEG. The TEG used the heat produced by a halogen bulb.

Later a prototype of the VLF (8.68 kHz) transmitter was developed shown on Fig. 12. This transmitter operated on the 1P24B vacuum tube and used an 55 mm diameter antenna coil. The transmitter is enclosed in a watertight containment. This prototype was successfully used for the underwater tests along with the large bandwidth transmitter described above.

Several radiation resistant sensors for in-core monitoring have been considered for the WSU. A variety of sensor is discussed in e.g. [2]. The sensor of interest for the current stage of the RADIO project is the thermocouple. This sensor type generates a temperature-dependent voltage. A standard K-type, nickel-alloy based chromel-alumel thermocouple is a passive sensor producing an open load voltage of about  $40 \mu\text{V}/^\circ\text{K}$ . This voltage needs to be amplified by an instrumentation amplifier with a high input impedance, to provide sufficient output voltage to modulate the oscillator, either by FM or AM methods. At later stage a broad range of sensors will be considered in the project. The list will include Self-Powered

Neutron Detectors (SPND), Linear Variable Differential Transformer (LVDT), pressure transducers, and gamma thermometers.

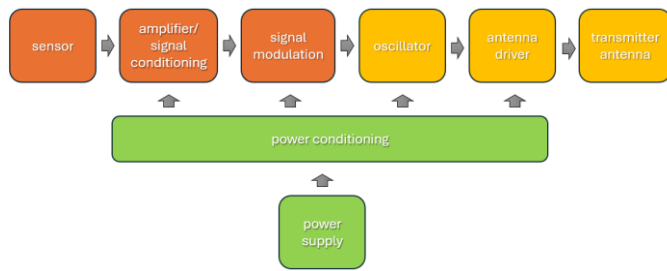


Fig. 11. Principal components of a wireless sensor unit (WSU)

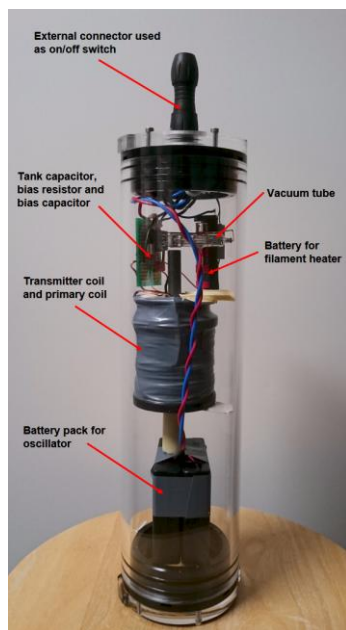


Fig. 12. Prototype low frequency oscillator design in a waterproof enclosure.

Another important element of the WSU is a TEG which provides electric power to the transmitter. The thermo-electric effect is widely applied in industry and consumer applications, with a large range of parts available on the market, either as TEG, or a Peltier cooling element. These commercial units can provide sufficient power for the application at hand, however, available heat, even if present in large quantities, can only be used if a sufficient large temperature difference can be maintained over both sides of the TEG, which can be limiting in small confined spaces [15]. The commercially available parts are usually based on bismuth telluride, as it provides one of the highest thermo-electric forces in the temperature range of interest ( $\sim 280 \mu\text{V}/^\circ\text{C}$ ). These parts come in standard size, e.g.  $30 \times 30$  or  $40 \times 40$  mm, with typically between 100 and 250 thermocouples and source resistances between 2 and 20 Ohm. TEGs with other semiconducting materials are available as well, e.g., half-Heusler materials, lead telluride (PbTe) and silicon-germanium (SiGe), but are not considered to have more favourable thermo-electric properties than the widely available bismuth telluride based TEGs [15]. Despite good performance of a commercial bismuth telluride in the gamma field of the GIF

facility it is still uncertain if semiconducting material would work under strong radiation fields as present in the HFR core. Alternatively, all-metal TEGs are considered. Nickel-alloy based thermocouples as chromel-alumel or chromel-constantan are a radiation resistant and widely used in nuclear instrumentation, but have smaller thermo-electric forces: about 40 and  $60 \mu\text{V}/^\circ\text{C}$ , respectively.

To produce the same output voltage as a bismuth-telluride based TEG, four to seven times more thermocouples are necessary. Alumel, chromel and constantan have a slightly higher thermal conductivity (about 30, 19, and  $20 \text{ W/m}\cdot\text{K}$ , respectively), compared to bismuth telluride, and an about one order of magnitude lower electrical resistivity (about 0.3, 0.7 and  $0.5 \mu\text{Ohm}\cdot\text{m}$  for alumel, chromel, and constantan, compared to roughly 6 to  $9 \mu\text{Ohm}\cdot\text{m}$  for bismuth telluride). The latter is relevant, because integration of a larger number of thermocouples on the same surface area will relevantly increase the source resistance of the TEG. However, since for obvious reasons thermo-couple-based TEGs are not available at the market, such a device must be designed and probably even built in-house.

Power conditioning is achieved by careful load matching of TEG and the oscillator. When combined with an instrumentation amplifier, additional power conditioning might be necessary.

## VI. CONCLUSIONS

A wireless in-core radio transmitter is currently under development at NRG-PALLAS. The transmitter will use vacuum tubes as active components and will be powered by means of a thermo-electric generator utilizing nuclear heating present in the core. The concept has been demonstrated in the proof-of-principle laboratory experiment.

In perspective of preparation of the future in-core irradiation test at HFR various components of the radio transmitter have been tested in the gamma irradiation facility in the spent fuel pool. Several irradiation tests have been carried from which one with on-line measurements.

The following conclusion on the suitability of the tested components and materials under gamma irradiation are made:

- The tested vacuum tubes showed good results during and after the irradiation and can be used in the future in-core irradiation, disregards the implementation version. It is unclear whether the reddish-brown colouring of the glass goes along with an embrittlement and may result in a potential failure of the tube's glass enclosure during harsher environmental conditions (heat, pressure, vibrations, neutron irradiation).
- Mica capacitors: both tested capacitors showed no change of the capacity after 690 kGy of irradiation, and no visual alterations were found.
- The polystyrene capacitor showed only a minor increase of the capacity after 690 kGy of irradiation.
- No changes were found at least for one type of a MLC capacitor.
- The three tested Ta-types are found unsuitable for the operation in a radiation field.
- No alterations were found for the tested wires and coils, showing that PU insulation and aliphatic polyamide bond

coatings are suitable isolation and bonding materials for the applied radiation conditions.

- It can be concluded that all tested resistors did not show any measurable alternation in the measured resistance.
- The Bismuth/Telluride TEG demonstrated perfect radiation resistance in contrast to the expectations. Both measured parameters, the Seebeck coefficient and internal resistance, did not show any degradation after the irradiation.

It was demonstrated that the highly electrically conductive wall of a reactor vessel presents a relevant barrier that determine the frequency range to be used and that can only be bridged by wireless technology at technical unfavourable very low frequencies (VLF). The results so far allow making first principal analyses of the signal attenuation to be expected in the HFR, or other reactor designs as the future Pallas reactor.

The results clearly show that reactor vessels made from less conductive metals than aluminium allow transmitting at technically more suitable frequencies, with less than 40 dB attenuation at 1 kHz.

It has been shown that in ultrapure water of the HFR basin transmission of magnetic waves proceeds without relevant attenuation.

Analyses of different components of the in-core Wireless Sensor Unit is presented. The current status of the different components of the WSU is summarized as follows:

- **Sensor:** As primary sensor for the current project, a thermocouple is considered, as routinely used in-core at the HFR and other reactors.
- **Signal modulation:** For signal modulation both AM and FM are been considered. No final selection of the method has been made.
- **Power supply:** Currently a commercial bismuth-telluride based TEG is selected as power source for the WSU. A TEG-powered oscillator built on vacuum tubes was successfully tested. Failure or insufficient performance would eventually leading to the need to design an all-metal TEG.
- **Transmitter antenna:** Several antenna designs have been tested. The designs include a proper matching to the oscillator, and considers the limited capacitance of available radiation resistant capacitors, and the limited space available in the GIF and HFR in-core positions.
- **Antenna driver:** The currently used oscillator design provides sufficient output current to directly drive the transmitter antenna.

### Acknowledgement

This research programme has been supported by the Dutch ministry of economic affairs and climate.

### REFERENCES

- [1] V. Agarwal, J.A. Smith, K.A. Manjunatha, "Assessing of Wireless Communication Technologies", Presentation on the Advanced Sensors and Instrumentation Annual Webinar, 29.10.2020 - 5.11.2020.
- [2] D. Xiang, "A Self-Powered, Wireless Sensor System for Remote and Long-Term Monitoring of Internal Conditions of Spent Nuclear Fuel Dry-Storage Casks", Presentation on the Advanced Sensors and Instrumentation Annual Webinar, 29.10.2020 - 5.11.2020
- [3] L. Zuo, "Self-Powered Wireless Through-wall Data Communication for Nuclear Environments", Presentation on the Advanced Sensors and Instrumentation Annual Webinar, 29.10.2020 - 5.11.2020.
- [4] T.J. Schröder, E. Rosca-Bocancea, "Current state of the art of wireless data transmission systems for repository monitoring", The 2nd international conference on Monitoring in Geological Disposal of Radioactive Waste, 9-11 April 2019, Paris, France.
- [5] T. J. Schröder, E. Rosca-Bocancea, "Wireless Data Transmission Demonstrator: from the HADES to the surface", MoDeRn Deliverable D.3.4.2, 2013.
- [6] J. Turso, J. V. Carvajal, S.C. Stafford, M.D. Heibel, P.M. Sirianni, M.M. Heagy, G. Corak, R.W. Flammang, N.G. Arlia, K. Unlu, 2020, "Toward the implementation of self-powered, wireless, real-time reactor power sensing", Annals of Nuclear Energy 139, 2020.
- [7] J. Carvajal, "Wireless Reactor Power Distribution Measurement System Utilizing an In-Core Radiation and Temperature Tolerant Wireless Transmitter and a Gamma-Harvesting Power Supply", DoE Advanced Sensors and Instrumentation Annual Webinar, 2020.
- [8] B. Sukhanov, A. Kireev, "Rod Tubes. Principle and design", Translation of an original Russian article published in July 1960 in the Russian Radio Magazine "Radio" by Dmitri Faguet; English proof-reading Joe Sousa, October 2011.
- [9] C.C. Phifer, "Radiation and Hydrogen in Glass", Sandia report SAND90 - 0950 - UC-404, 1990.
- [10] D. Ehr, P. Ebeling, "Radiation defects in borosilicate glasses", Glass Technol., 44 (2), p.46-49, 2003.
- [11] H.J. Reich, "Theory and Application of Eletron Tubes", 2nd ed., McGraw-Hill, 1944.
- [12] J. Deketh, "Fundamentals of Radio-Valve Technique". N.V. Philips' Gloeilampenfabrieken, 1949.
- [13] Dood, C.V., W.E. Deeds, 1968, Analytical Solutions to Eddy-Current Probe-Coil Problems, Journal of Applied Physics, 39(6), p.2829-2838.
- [14] T.J. Schröder, "Low frequency data transmission by magnetic induction", NRG note 24831/21.229319, 15 December 2021.
- [15] T.J. Schröder, E. Rosca-Bocancea, J. Hart, "Thermal energy harvesting from High-Level Waste", The 2nd international conference on Monitoring in Geological Disposal of Radioactive Waste, 9-11 April 2019, Paris, France.